A COMPARATIVE NEUTRONICS ANALYSIS BY USING ENDF/B-VI AND JEF2.2 LIBRARIES FOR THE ENHS BENCHMARK PROBLEM

Ser Gi Hong, Yeong Il Kim, and Young Jin Kim
Korea Atomic Energy Research Institute
Duckjin-dong, Yusong-gu, Taejon, Korea
hongsg@kaeri.re.kr ; yikim1@kaeri.re.kr ; youkim@kaeri.re.kr

ABSTRACT

In this paper, as a preliminary work of the ENHS (Encapsulated Nuclear Heat Source) core design, the ENHS benchmark problem is analyzed with two nuclear data libraries (ENDF/B-VI, JEF2.2) processed by NJOY and TRANSX. The basic core physics data are calculated by using the TWODANT and DIF3D codes. The depletion analysis is performed by using REBUS-3. From the analysis, it is shown that there is a significant discrepancy in eigenvalue between ENDF/B-VI and JEF2.2 and that the eigenvalue evolution over burnup is sensitive to the division of the core zone for depletion analysis. It seems that this large discrepancy is due to the larger value of capture cross sections of the heavy isotopes in JEF2.2. For the reactivity worth and the temperature reactivity coefficients, there are comparatively good agreements between two data libraries.

1. INTRODUCTION

Recently, the Encapsulated Nuclear Heat Source (EHNS) reactor, which is a new Pb or Pb-Bi cooled highly modular fast spectrum concept has been studied through an international cooperation [1~8]. The ENHS reactor featured 20 years of operation without refueling, no fuel shuffling, and 100% natural circulation eliminating the need for primary and secondary coolant pumps. From the view point of core physics, the reactor core having a uniform fuel composition of metallic Pu-U-Zr(10w/o) or U-Zr(10w/o) is designed to have the nearly zero burnup reactivity swing (<0.5%) over 20 EFPY without any fuel handling and to have the good temperature feedback characteristics. As a preliminary step of the detailed ENHS core design, benchmarking of the computational codes including computational methodologies and nuclear data is very important to assess the relative accuracies of the core design tools. In fact, during last year, there have been some efforts for benchmarking of the computational tools and nuclear data [1,9]. The accompanying paper treats more detailed comparative study with different nuclear data and different computer codes on the ENHS benchmark problem [10]. In this paper, a comparative neutronics analysis by using two nuclear data libraries (ENDF/B-VI, JEF2.2) that are processed by NJOY and TRANSX is performed and the results are inter-compared [9]. The results show that there is a significant discrepancy (~ 2.0%) in eigenvalue between ENDF/B-VI and JEF2.2. This large discrepancy may be related to the fact that the effective one group capture cross sections of heavy isotopes (plutonium and uranium) estimated by JEF2.2 are considerably larger than those by ENDF/B-VI. Their eigenvalue evolution curves over 30 years are approximately parallel to each other. And these eigenvalue evolution curves are sensitive to the division methods of the core zone for depletion analysis. Therefore, to obtain reasonable accuracy of the eigenvalue, the core region should be divided into a sufficient number of depletion zones. In section 2, the ENHS

benchmark problem and computer code systems used in this work are described. Section 3 summaries the analysis results and the section 4 describes the conclusions.

2. PROBLEM DESCRIPTION AND CORE DESIGN METHODS

The core model consists of twenty-four fuel assemblies having 217 rods in a hexagonal array [1]. The core was designed to generate 250MW thermal power at the average heat generation rate of 120W/cm. The core height is 4m and the lattice pitch-to-diameter is 1.15. The fuel pin radius and the clad thickness are 0.5cm and 0.1cm, respectively. The central assembly site is reserved for a safety rod assembly. Since this central site is filled with Pb coolant during reactor operation, we calculated for this case. The Pb surrounding the core serves the reflector. The density of Pb is calculated by 11.072-0.0012*T (g/cc) for temperature from 400 to 700C. All fuel rods are of a uniform composition. The fuel is a metallic alloy of U-Pu-10%Zr. The initial plutonium enrichment is 10.9%. The fuel density is assumed to be 75% of the nominal density and its nominal density is 15.85g/cc. The uranium is 0.2w/o depleted U-235 and the initial plutonium is from LWR spent fuel : the weight percents of the isotopes Pu-239, 240, 241, and 242 are 67.2, 21.7, 6.4, and 4.7, respectively. The clad and structural material is the stainless steel having 64.8w/o Fe, 17.0w/o Cr, 14.0w/o Ni, 2.8w/o Mo, and 1.5w/o Mn. The nominal density of the stainless steel is assumed to be 7.95g/cc. The radial reflector assembly includes a voided container (10.0v/o stainless steel) that is 15cm thick and as long as the fuel section in the core. The core model for neutronics calculation is a R-Z homogeneous geometry. The core model including surrounding regions is given in Figure 1. The material compositions and their atomic number densities are given in Table I and II, respectively.

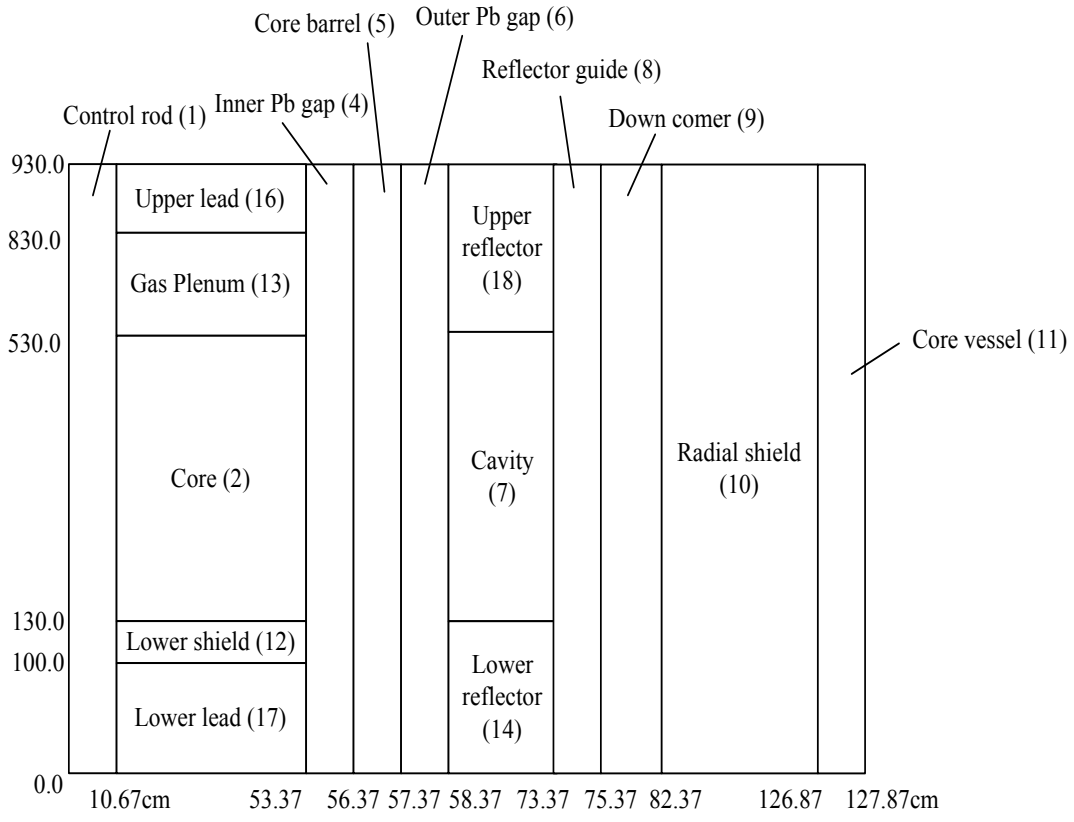

Figure 1. Configuration of the ENHS benchmark problem

Table I. Material compositions for the ENHS benchmark problem

Regions (region number)	Material, volume fraction	Temperature (K)
Control rod region (1)	99%Pb + 1%SS	753
Core (2)	47.621%fuel+31.4253%Pb +20.953%SS	753
Inner Pb gap (4)	100%Pb	753
Core barrel (5)	100%SS	753
Outer Pb gap (6)	100%Pb	693
Cavity (7)	100%Pb (or 10%SS[a])	693
Reflector guide (8)	70%Pb+30%SS	693
Down comer (9)	100%Pb	693
Radial shield (10)	100%Pb	693
Core vessel (11)	100%SS	693
Lower shield (12)	100%Pb	693
Gas plenum (13)	31.4253%Pb+20.953%SS	813
Lower reflector (14)	100%Pb	693
Upper Pb (16)	100%Pb	813
Lower Pb (17)	100%Pb	693
Upper reflector (18)	90%Pb+10%SS	693

[a]Lead is not filled

Table II. Atomic number densities for composing materials

Regions (region number)	Atomic number density (atoms/barn-cm)
Control rod region (1)	Pb : 3.02043E-2, Fe : 5.55118E-4, Ni : 1.14172E-4, Cr : 1.56540E-4, Mo : 1.37239E-5, Mn : 1.30727E-5
Core (2)	Pu-239 : 9.40189E-4, Pu-240 : 3.02336E-4, Pu-241 : 8.87696E-5, Pu-242 : 6.49405E-5, U-235 : 2.32633E-5, U-238 : 1.14617E-2, Zr : 3.73749E-3, Pb : 9.58770E-3, Fe : 1.16316E-2, Ni : 2.39230E-3, Cr : 3.28003E-3, Mo : 2.87562E-4, Mn : 2.73916E-4
Inner Pb gap (4)	Pb : 3.05094E-2
Core barrel (5)	Fe : 5.55118E-2, Ni : 1.14172E-2, Cr : 1.56540E-2, Mo : 1.37239E-3, Mn : 1.30727E-3
Outer Pb gap (6)	Pb : 3.07187E-2
Cavity (7)	Pb : 3.07187E-2
Reflector guide (8)	Pb : 2.15031E-2, Fe : 1.66535E-2, Ni : 3.42517E-3, Cr : 4.69619E-3, Mo : 4.11718E-4, Mn : 3.92180E-4
Down comer (9)	Pb : 3.07187E-2
Radial shield (10)	Pb : 3.07187E-2
Core vessel (11)	Fe : 5.55118E-2, Ni : 1.14172E-2, Cr : 1.56540E-2, Mo : 1.37239E-3, Mn : 1.30727E-3
Lower shield (12)	Pb : 3.07187E-2
Gas plenum (13)	Pb : 9.52193E-3, Fe : 1.16316E-2, Ni : 2.39230E-3, Cr : 3.28003E-3, Mo : 2.87562E-4, Mn : 2.73916E-4
Lower reflector (14)	Pb : 3.07187E-2
Upper Pb (16)	Pb : 3.03001E-2
Lower Pb (17)	Pb : 3.07187E-2
Upper reflector (18)	Pb : 2.76468E-2, Fe : 5.55118E-3, Ni : 1.14172E-3, Cr : 1.56540E-3, Mo : 1.37239E-4, Mn : 1.30727E-4

We used the REBUS-3 [11]/DIF3D [12] code system for depletion analysis while the basic core physics data were calculated with DIF3D and TWODANT [13]. The JEF2.2 based nuclear library called KAFAX-F22 [14] is a 80 group cross section library (MATXS format) and the ENDF/B-VI based nuclear library called KAFAX-E66 [15] is a 150 group cross section library (MATXS format). These two multigroup cross section libraries containing the microscopic cross section and self-shielding data for master nuclides excluding fission products as a function of temperature are the starting point for master nuclides. For fission products, the starting point is a ENDF/B-VI (JENDL-3.2 based for some seven nuclides) based 80 group cross section library (MATXS format) that contains microscopic cross sections for fission products [16]. In fast breeder reactor analysis, the fission products for each fissionable isotope generally are lumped into a single fictitious or lumped fission product by weighting with fission yield (ENDF/B-VI based). In this paper, the 17 lumped fission products and one dummy isotope are used to model the 172 fission products. The MATXS format nuclear libraries by using the TRANSX code [17] are transformed into the ISOTXS format that can be used in DIF3D and TWODANT. For both nuclear libraries, the depletion analysis are performed with the 80 or 9 group cross section sets that are prepared by using the 150 group core spectrum for ENDF/B-VI, 80 group core spectrum for JEF2.2, and TRANSX. The space dependent effect of isotopic depletion is analyzed by changing the zone division method. In each zone, the atomic number densities are assumed to be spatially constant.

3. ANALYSIS RESULTS

Before the depletion calculation proceeds, it is important that the basic core physic parameters are estimated at BOL. The results are given in Table III. The percent error of eigenvalues between TWODANT (25group) and MCNP (UCB results) [1] is approximately 0.2%. It is considered that this error is due to the differences in cross section processing and the computational methods (deterministic, stochastic transport). However, the discrepancy between JEF2.2 and ENDF/B-VI is large (nearly 2.0%). This is due to the larger capture cross section of the important heavy isotopes in JEF2.2 (See Table V). Other quantities including conversion ratio, core void reactivity (100% voided), reflector worth, and cold-to-hot reactivity swing show good agreements, comparatively.

Table III. Basic core physic parameters at BOL

Parameters	KAERI (ENDF/B-VI)	KAERI (JEF2.2)	UCB (ENDF/B-VI)
Initial conversion ratio	1.1764	1.1819	1.1629
Reflector worth (dk)	+0.0272	+0.0262	+0.0232
Void reactivity (core, dk)	+0.0194	+0.0218	+0.0194
Initial DIF3D k_{eff}	1.010295 (150g)	0.988721	-
Initial TWODANT k_{eff}	1.0126089 (25g)	0.990984	1.015 (MCNP)
Cold-to-hot swing (dk)	-0.00443	-0.00494	-0.00466

The temperature reactivity coefficients at BOL and EOL are compared in Table IV(a) and IV(b), respectively. All temperature reactivity coefficients are negative for both JEF2.2 and ENDF/B-VI. The total cold-to-hot reactivity swing is -0.4 ~ -0.5%. In calculating the temperature reactivity coefficients, the following four effects are considered separately : (a) coolant expansion, (b) thermal axial expansion of fuel rods, (c) thermal radial expansion of the core support structure, (d) Doppler effect. The cold temperatures for all effects are 480C at nominal condition and 350C at startup. In the calculation of the cold-to-hot swing, the hot temperatures for Doppler effect and for the rest are 700C and 480C, respectively. At nominal condition, the hot temperatures for Doppler and the rest are 700C and 600C, respectively. The results show that the temperature reactivity coefficients estimated by JEF2.2 except the coolant density change effect are slightly larger in absolute value than those estimated by ENDF/B-VI. The temperature reactivity coefficients except the axial expansion of fuel

rods becomes less negative at EOL. The void reactivity and the reflector worth at BOL and EOL are compared in Table IV(c). Although the results estimated by two data libraries show good agreements, it is shown that the void reactivity estimated by JEF2.2 is slightly more positive than those by ENDF/B-VI. The voidings in inner 1/3 core and middle 1/3 core give positive reactivity while the voiding in outer 1/3 core gives negative one because the negative effect by increase of neutron leakage is more dominant than the positive effect by spectrum hardening in outer 1/3 region. The void reactivities and the reflector worth are slightly degraded at EOL in comparison with those at BOL.

Table IV(a) Temperature reactivity coefficients at BOL

Effects	Cold-to-hot (dk)		At nominal condition (dρ/dT)	
	ENDF/B-VI	JEF2.2	ENDF/B-VI	JEF2.2
Pb expansion	-4.864E-04	-4.181E-04	-4.2964E-06	-4.1729E-06
Axial expansion of fuel rod	-8.682E-04	-8.389E-04	-6.3128E-06	-6.3725E-06
Radial expansion of grid plate	-9.147E-04	-9.196E-04	-7.1223E-06	-7.4482E-06
Doppler	-2.1605E-03	-2.7668E-03	-6.4164E-06	-7.1575E-06
Total summation	-4.4298E-03	-4.9434E-03	-	-

Table IV(b) Temperature reactivity coefficients at EOL

Effects	Hot-to-cold (dk)		At nominal condition (dρ/dT)	
	ENDF/B-VI	JEF2.2	ENDF/B-VI	JEF2.2
Pb expansion	-4.454E-04	-3.699E-04	-3.6851E-06	-3.1862E-06
Axial expansion of fuel rod	-7.569E-04	-7.526E-04	-6.5240E-06	-6.5334E-06
Radial expansion of grid plate	-4.069E-04	-4.266E-04	-3.3718E-06	-3.6673E-06
Doppler	-1.3995E-03	-1.7955E-03	-4.0285E-06	-4.4913E-06
Total summation	-3.0078E-03	-3.3446E-03	-	-

Table IV(c) Void reactivities and reflector worth (dk) at BOL and EOL

	ENDF/B-VI	JEF2.2
BOL		
Void reactivity (dk)		
Inner 1/3 core	+0.015318	+0.016117
Middle 1/3 core	+0.006228	+0.007032
Outer 1/3 core	-0.0018407	-0.0012646
Whole core	+0.0194	+0.0218
Reflector worth (dk)	+0.0272	+0.0262
EOL		
Void reactivity (dk)		
Inner 1/3 core	+0.015162	+0.016838
Middle 1/3 core	+0.006981	+0.008573
Outer 1/3 core	-0.001634	-0.0002394
Whole core	+0.020171	+0.023226
Reflector worth (dk)	+0.0258	+0.0244

The eigenvalue evolutions over time for lead and steel cavity cases are compared in Fig. 2 and 3, respectively. The eigenvalues for all cases increase initially and then decrease. This initial increase of eigenvalue is due to the formation of Pu-239 (this is a main fissile material) resulting from the neutron capture of U-238. The initial eigenvalues except JEF2.2 agree fairly with one another. Fig. 2 and 3 show that there are significant differences in trends of eigenvalue change versus time for three zone division methods of core region and that the eigenvalue evolution curves by ENDF/B-VI and JEF2.2

with single zone for core are parallel to each other. As the core region is refined, the eigenvalue after its maximum value decreases more rapidly. Therefore, to obtain reasonable accuracy of the eigenvalue evolution, the core region should be divided into a sufficient number of depletion zones. However, it is noted that the number of energy groups has small effect both on the trend of eigenvalue versus time and on the initial eigenvalue. The eigenvalues by KAERI (ENDF/B-VI, 9zones) and ANL(ENDF/B-V) show fairly good agreement. The ANL 230group cross section set [18] was obtained by using MC^2 and ENDF/B-V.2. All calculation of core physics parameters and depletion analysis were performed by DIF3D, REBUS-3, and the 230 group cross sections. Table V shows the effective one group cross sections (fission and capture) of the important heavy isotopes. It is noted that JEF2.2 gives considerably larger capture cross sections than ENDF/B-VI. Table VI(a) shows the time integrated region average burnup (GWD/MTH) for ENDF/B-VI (80group, 9zones), ENDF/B-VI(9group, 9zones), and JEF2.2(80groups, 9zones). The results show that three method gives nearly the same values of the burnup. The peak burnup values at 30 years are also nearly the same.

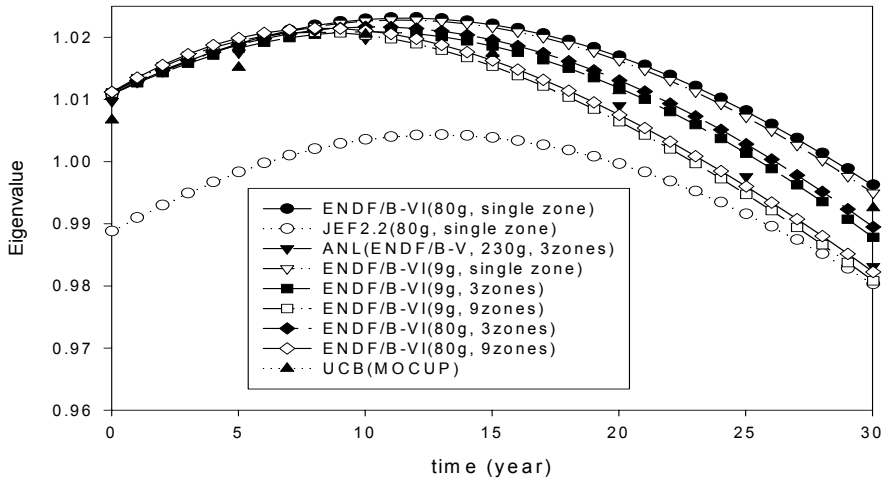

Figure 2. Comparison of the eigenvalue evolutions (lead cavity case)

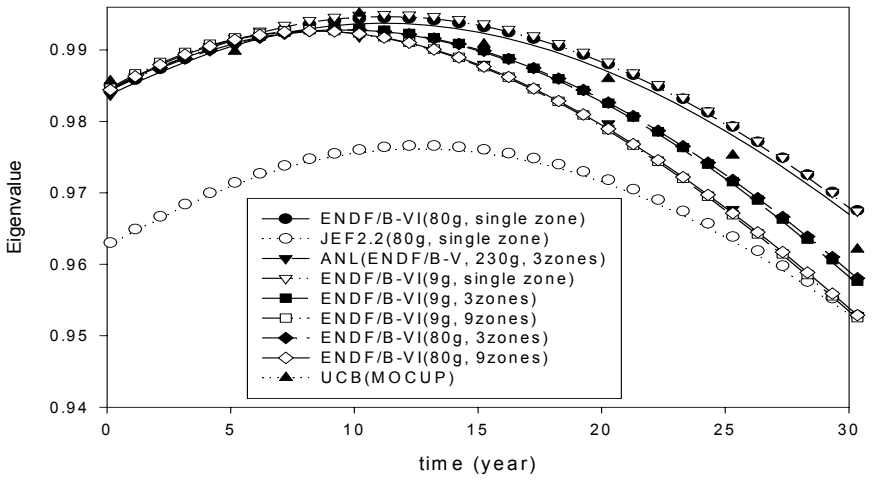

Figure 3. Comparison of the eigenvalue evolutions (steel cavity)

Table V. Comparison of the one group effective cross sections

Nuclides	Capture			Fission		
	KAERI (ENDF/B-VI)	KAERI (JEF2.2)	ANL (ENDF/B-V)	KAERI (ENDF/B-VI)	KAERI (JEF2.2)	ANL (ENDF/B-V)
Pu-239	.3093	**.3487**	0.3128	1.6579	1.6741	1.678
Pu-240	.3679	**.4114**	0.3740	.3854	.3526	0.3858
Pu-241	.3186	**.4627**	0.3311	2.1266	2.1766	2.109
Pu-242	.3226	**.3462**	0.3858	.2690	.2421	0.2732
U-235	.3957	**.4054**	0.4074	1.5954	1.6197	1.586
U-238	.2072	**.2143**	0.2126	.0334	.0309	0.0339
FPU235	.1958	.2017	0.2393			
FPU238	.2605	.2659	0.3026			
FPPU239	.2828	.2893	0.3330			
FPPU240	.2955	.3013	0.3452			
FPPU241	.3020	.3131	0.3593			
Np-237	1.1278	1.1736	1.138	.3371	.3005	0.3581
Am-241	1.2225	1.5675	1.282	.2587	.2247	0.2785
Am-242m	.2360	.4321	0.2269	3.2401	2.7459	3.178
Am-243	1.1053	1.3208	0.9512	.1869	.1723	0.2206
Cm-242	.1912	.3479	0.1815	.1454	.5779	0.1470
Cm-243	.1628	.1511	0.1566	2.2309	2.8921	2.178
Cm-244	.6421	.4554	0.6237	.4411	.4009	0.4424
Cm-245	.2385	.2431	0.2384	1.9339	2.3084	2.329
Cm-246	.1675	.1725	0.1616	.2640	.2324	0.2638

The core region peak fast fluences (>0.1MeV, 10^{23} n/cm^2) are compared in Table VI(b). The results show that three method gives nearly the same values of the core region peak fast fluence. Finally, the ratios of the number densities (atoms/barn-cm) of the heavy metals between ENDF/B-VI and JEF2.2 are compared in Table VII. It is noted that the ratios are between 0.91 and 1.02 for important fissile and fertile isotopes while there are relatively larger deviations in the other isotopes including minor actinides.

Table VI(a). Time dependent integrated region average burnup (KAERI, GWD/MTH)

Year	Inner region			Middle region			Outer region			Core average		
	A[a]	B[b]	C[c]	A	B	C	A	B	C	A	B	C
5	31.644	31.770	31.589	27.705	27.809	27.639	21.833	21.727	21.788	25.607	25.613	25.555
10	63.337	63.529	63.260	55.382	55.556	55.255	43.749	43.581	43.651	51.252	51.265	51.149
15	94.882	95.103	94.795	83.005	83.228	82.824	65.804	65.604	65.652	76.920	76.939	76.771
20	126.18	126.41	126.09	110.56	110.82	110.33	88.021	87.811	87.814	102.60	102.62	102.41
25	157.20	157.41	157.10	138.04	138.33	137.77	110.41	110.20	110.15	128.28	128.31	128.04
30	187.89	188.07	187.80	165.45	165.74	165.13	132.97	132.78	132.65	153.96	154.01	153.68
30 (peak)	250.37	250.15	250.94	237.57	237.22	237.92	198.10	198.79	198.08	220.93	221.10	221.15

[a]ENDF/B-VI(80g, 9zones), [b]ENDF/B-VI(9g, 9zones), [c]JEF2.2(80g, 9zones)

Table VI(b). Core region peak fast fluence (>0.1MeV, 10^{23}n/cm^2, KAERI)

Time (year)	Inner region			Middle region			Outer region			Core average		
	A[a]	B[b]	C[c]	A	B	C	A	B	C	A	B	C
5	1.831	1.808	1.796	1.698	1.681	1.663	1.298	1.289	1.268	1.530	1.516	1.498
10	3.665	3.615	3.598	3.399	3.362	3.331	2.598	2.579	2.540	3.063	3.032	2.999
15	5.463	5.383	5.361	5.068	5.009	4.965	3.877	3.847	3.789	4.568	4.519	4.472
20	7.204	7.095	7.063	6.689	6.608	6.547	5.124	5.086	5.003	6.031	5.965	5.899
25	8.896	8.759	8.711	8.267	6.166	8.081	6.342	6.295	6.184	7.456	7.375	7.284
30	10.58	10.42	10.35	9.849	9.731	9.618	7.564	7.512	7.368	8.885	8.791	8.671

[a]ENDF/B-VI(80g, 9zones), [b]ENDF/B-VI(9g, 9zones), [c]JEF2.2(80g, 9zones)

Table VII. Ratio of atomic number density (ENDF/B-VI / JEF2.2)

Isotopes	0 year	5 year	10 year	15 year	20 year	25 year	30 year
U-234	1.000E+00	8.347E-01	8.210E-01	8.183E-01	8.168E-01	8.152E-01	8.131E-01
U-235	1.000E+00	1.006E+00	1.011E+00	1.014E+00	1.016E+00	1.018E+00	1.018E+00
U-236	1.000E+00	9.837E-01	9.976E-01	1.011E+00	1.023E+00	1.035E+00	1.047E+00
U-238	1.000E+00	1.001E+00	1.002E+00	1.002E+00	1.003E+00	1.003E+00	1.004E+00
PU238	1.000E+00	8.245E-01	8.198E-01	8.200E-01	8.194E-01	8.180E-01	8.158E-01
NP237	1.000E+00	9.166E-01	9.149E-01	9.142E-01	9.138E-01	9.138E-01	9.140E-01
PU239	1.000E+00	9.967E-01	9.959E-01	9.962E-01	9.968E-01	9.976E-01	9.986E-01
PU240	1.000E+00	9.839E-01	9.705E-01	9.596E-01	9.507E-01	9.434E-01	9.373E-01
PU241	1.000E+00	9.992E-01	9.831E-01	9.595E-01	9.358E-01	9.157E-01	9.004E-01
PU242	1.000E+00	9.758E-01	9.587E-01	9.442E-01	9.307E-01	9.176E-01	9.044E-01
AM241	1.000E+00	1.025E+00	1.044E+00	1.057E+00	1.066E+00	1.071E+00	1.073E+00
AM242M	1.000E+00	7.805E-01	7.844E-01	7.859E-01	7.853E-01	7.836E-01	7.811E-01
AM243	1.000E+00	9.190E-01	9.166E-01	9.149E-01	9.128E-01	9.103E-01	9.072E-01
CM242	1.000E+00	8.041E-01	8.229E-01	8.347E-01	8.415E-01	8.454E-01	8.476E-01
CM243	1.000E+00	4.472E-01	4.715E-01	4.917E-01	5.075E-01	5.197E-01	5.290E-01
CM244	1.000E+00	7.498E-01	7.406E-01	7.337E-01	7.280E-01	7.226E-01	7.174E-01
CM245	1.000E+00	1.062E+00	1.070E+00	1.079E+00	1.089E+00	1.096E+00	1.103E+00
CM246	1.000E+00	1.025E+00	1.032E+00	1.041E+00	1.052E+00	1.061E+00	1.069E+00

4. CONCLUSIONS

In this paper, an analysis for the ENHS neutronics benchmark problem was performed with ENDF/B-VI and JEF2.2 nuclear data libraries. The TRANSX code was used to prepare the multigroup cross sections that is the ISOTXS format and usable in diffusion and transport solvers. The depletion analysis was performed by using the REBUS-3/DIF3D code. There was large discrepancy in the initial eigenvalues between ENDF/B-VI and JEF2.2. It seems that this large discrepancy is due to the large difference in the capture cross sections of the heavy isotopes. For ENDF/B-VI, the BOL eigenvalue estimated by TWODANT agrees fairely with that by MCNP at UCB. In the depletion calculation, the effects of the number of energy groups (i.e., condensation effect) and the number of the depletion zones divided were analyzed. From the analysis, it is found that the condensation of the energy group has small effect on the results of the depletion calculations while the zone division for the space dependent depletion has significant effect on the results (particularly on the eigenvalue evolution). For the reactivity worth including the temperature reactivity coefficients and the void reactivities, JEF2.2 and ENDF/B-VI give comparatively good agreements.

ACKNOWLEDGEMENTS

This work was supported by the Nuclear Energy Research Initiative Project of Korean Ministry of Science and Technology (MOST).

REFERENCES

1. E. Greenspan, H. Shimada, K. Wang, “Long-Life Cores with Small Reactivity Swing,” *Proc. ANS. Int. Topl. Mtg. Advances in Reactor Physics and Mathematics and Computation into Next Millennium (PHYSOR2000)*, May 7-12, 2000.
2. E. Greenspan, N. W. Brown, M. D. Carelli et al., “The Encapsulated Nuclear Heat Source – A Generation IV Reactor,” *Proceedings of GLOBAL 2001*, Paris, France, Sept. 9-13, 2001.
3. E. Greenspan et. al., “The Encapsulated Nuclear Heat Source Reactor Concept,” *Trans. Am. Nucl. Soc.*, **85**, p.71 (2001).
4. E. Greenspan et al., “The Encapsulated Nuclear Heat Source Potential for Meeting Generation IV Goal,” *Trans. Am. Nucl. Soc.*, **85**, p.73 (2001).

5. D. C. Wade et al., "ENHS : The Encapsulated Nuclear Heat Source – A Nuclear Energy Concept for Emerging Worldwide Energy Markets," *Proc. of ICONE 10 : Tenth Int. Conf. on Nuclear Engineering*, Arlington, Virginia USA, April 14-18, 2002.
6. E. Greenspan et al., "The Long-Life Core Encapsulated Nuclear Heat Source (ENHS) Generation IV Reactor," to be presented at *Int. Cong. on Advanced Nuclear Power Plants (ICAP*P), Hollywood, Florida, 2002.
7. S. G. Hong, E. Greenspan, and Y. I. Kim, "Once-for-Life Core for the Encapsulated Nuclear Heat Source (ENHS) reactor," to be presented at *ANS 2002 Annual Meeting*, Hollywood, Florida, 2002.
8. S. G. Hong, E. Greenspan, and Y. I. Kim, "A Once for Life Core Design for the Encapsulated Nuclear Heat Source (ENHS) Reactor," These Proceedings
9. S. G. Hong and Y. I. Kim, "Comparison of the ENDF/B-VI and JEF2.2 Nuclear Data for the ENHS Benchmark Problem," *Trans. Am. Nucl. Soc*., **85**, p.111 (2001).
10. M. Milosevic' et al., "The ENHS Benchmarks," These Proceedings.
11. K. L. Derstine, "DIF3D : A Code to Solve One-, Two-, and Three-Dimensional Finite-Difference Diffusion Theory Problems," ANL-82-64, Argonne National Laboratory (April 1984).
12. B. J. Toppel, "User's Guide for the REBUS-3 Fuel Cycle Analysis Capability," ANL-83-2, Argonne National Lab. (Mar. 1983).
13. R. E. Alcouffe, et al., "User's Guide for TWODANT : A Code Package for Two-Dimensional Diffusion-Accelerated, Neutral-Particle Transport," LANL report, LA-10049-M (1984).
14. J. D. Kim and C. S. Gil, "KAFAX-F22 : Development and Benchmark of Multigroup Library for Fast Reactor Using JEF2.2," KAERI/TR-842/97, KAERI (1997).
15. J. D. Kim, "KAFAX-E66," Calculation Note No. NDL-23/01, Nuclear Data Evaluation Lab. Internal Report, Korea Atomic Energy Research Institute (2001).
16. J. D. Kim, "Generation of Lumped Fission Product Cross Sections for Fast Reactors," NDL-25/99, Korea Atomic Energy Research Institute (1999).
17. R. E. MacFarlane, "TRANSX 2 : A Code for Interfacing MATXS Cross Section Libraries to Nuclear Transport Codes," LA-12312-MS, Los Alamos National Lab. (Dec. 1993).
18. K. N. Grimm, "ENHS Neutronics Benchmark – Argonne Results," ANL Intra-Laboratory Memo, 2000.